Joint Optimization of Role Switching and Trajectory Planning for Multi-UAV Assisted Uplink Secure Communications

Chengzhe Zhang†, Guanxiong Zheng†, Wenqian Cao†, and Yi Zhang†*

†Department of Information and Communication Engineering, School of Informatics, Xiamen University, China
* Corresponding Author: yizhang@xmu.edu.cn

***Abstract*—As an aerial base station, unmanned aerial vehicles (UAVs) offer significant potential to enhance terrestrial communications due to their flexible on-demand deployment, enabling rapid and reliable line-of-sight (LoS) wireless connectivity. This paper investigates a multi-UAV-assisted uplink wireless communication network under eavesdropping threats with location uncertainty. The proposed system enhances operational sustainability through energy replenishment stations while introducing multi-role UAVs capable of dynamic role-switching among three functions: communication reception, friendly jamming, and energy replenishment. To maximize worst-case secrecy capacity, we formulate a joint optimization problem encompassing UAV role-switching decisions, power allocation, and trajectory planning. By decomposing this multi-variable optimization problem into tractable subproblems, we derive a globally optimal solution through an iterative framework based on block coordinate descent (BCD) and successive convex approximation (SCA). Simulation results confirm that the proposed algorithm outperforms existing benchmarks in improving secrecy capacity.**

***Index Terms*—Secure communication, eavesdropping, friendly jamming, power allocation.**

I. Introduction

Due to the compact size, high mobility, and flexible deployment capabilities, unmanned aerial vehicles (UAVs) can act as aerial base stations to extend ground network coverage by quickly establishing line-of-sight (LoS) communication links, especially where terrestrial infrastructure is limited, such as obstructed environments, long-distance communication, or natural disasters [1]. Despite these advantages, UAVs operating in open wireless environments are vulnerable to physical interception, which poses serious security threats to the confidentiality of wireless transmissions [2], [3]. Although traditional encryption techniques can offer protection, they require high computational complexity and energy consumption, constraints that UAVs cannot afford. As an alternative, *physical layer security (PLS)* is proposed to leverage wireless channel randomness for efficient eavesdropping prevention.

The deployment of UAVs as *friendly jammers* has emerged as an effective method to secure wireless links. By exploiting their mobility and LoS characteristics, friendly jamming UAVs can transmit artificial noise based on the channel state information (CSI) of both the legitimate users and potential eavesdroppers, thereby improving secrecy performance. In [4], a bidirectional secure communication system assisted by dual UAVs is investigated, where the trajectories of both the information UAV and the friendly jammer, along with the transmit power, are jointly optimized to maximize the worst-case average secrecy capacity. In [5], Zhang et al. propose two secure data collection schemes involving cooperation between an information UAV and a friendly jammer. These schemes jointly optimize UAV trajectories, velocities, user scheduling, and transmitting power to maximize the worst-case average secrecy capacity and secrecy energy efficiency.

Although UAVs are effective in countering eavesdropping when serving as jammers to interfere with eavesdroppers, their fixed roles limit the flexibility of deployment. Enabling *role switching* within a single UAV can enhance trajectory adaptability and potentially improve secure communication performance. In [6], Hou et al. propose a UAV-enabled covert federated learning framework, where the UAV not only coordinates federated learning operations but also transmits artificial noise to interfere with eavesdroppers. In [7], the authors propose a scheme in which the UAV's transmit power is divided into two parts, dedicated to confidential information transmission and artificial noise generation, respectively. Most existing studies consider only single-UAV secure communication scenarios. The limited coverage and poor robustness of a single UAV makes it unsuitable for multi-user, multi-eavesdropper scenarios [8], leaving the problem of secure communication in such settings largely unexplored.

Basing on the above surveys and motivations, we study a multi-UAV assisted uplink secure communication network with the presence of eavesdropping threats. Some energy replenishment stations are deployed to extend the operational time of the UAVs due to their limited battery capacities [9]. To counteract these threats, a new type of multi-role UAV is proposed with dynamic role-switching capabilities among communication reception, friendly jamming, and energy replenishment operations. A secrecy capacity maximization problem is modeled by considering the practical constraints, including limited battery capacity of UAVs, imperfect knowledge of eavesdropper locations, and the presence of no-fly zones (NFZ). The multi-UAV deployment method is pro-

This work was supported by the National Natural Science Foundation of China under Grants 62401485 and the Fundamental Research Funds for the Central Universities of China under Grants 20720250028.

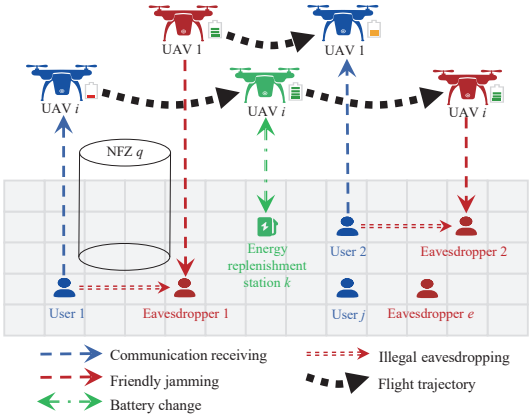

Fig. 1. Multi-UAV assisted uplink secure communication network.

posed to maximize the secrecy capacity by jointly optimizing UAV role-switching decisions, power allocation strategies, and trajectory planning while maintaining the UAV's energy above a safe threshold. Besides, a secure communication deployment algorithm is developed based on BCD and SCA, tailored to the structure of the formulated problem. The simulation results confirmed that the proposed DOFJ demonstrates excellent performance in terms of secrecy capacity.

II. System Model and Problem Formulation

The proposed multi-UAV assisted uplink secure communication network is illustrated in Fig. 1, which consists of mutiple UAVs $\{1,\ldots,i,\ldots,I\}$, multiple ground users $\{1,\ldots,j,\ldots,J\}$, some potential eavesdroppers $\{1,\ldots,e,\ldots,E\}$, and some energy replenishment stations $\{1,\ldots,k,\ldots,K\}$. The total time T is uniformly discretized into N time slots, that is, $\{1,\ldots,n,\ldots,N\}$. The duration of each time slot is $\delta t = T/N$, which is small enough so that the position of UAV can be considered fixed in each time slot. To counter eavesdropping, a multi-role UAV with dynamic role switching is introduced. All devices in the scenario are equipped with one antenna. The system adopts Orthogonal Frequency Division Multiple Access (OFDMA), where each user occupies a specific subcarrier and the UAV is equipped with only one transceiver [10].

The coordinates are $\mathbf{w}_j = (x_j, y_j)^{\mathrm{T}}$, $\mathbf{w}_k = (x_k, y_k)^{\mathrm{T}}$ and $\mathbf{w}_e = (x_e, y_e)^{\mathrm{T}}$. The estimated value and the estimation error of $\mathbf{w}_e$ are $\hat{\mathbf{w}}_e = (\hat{x}_e, \hat{y}_e)^{\mathrm{T}}$ and $\Delta\mathbf{w}_e = (\Delta x_e, \Delta y_e)^{\mathrm{T}}$, which satisfy: $\mathbf{w}_e = \hat{\mathbf{w}}_e + \Delta\mathbf{w}_e$ and $\|\Delta\mathbf{w}_e\|^2 \le r_{eve}^2$, r_{eve} represents the radius of the circular uncertain region where the actual position is $\mathbf{w}_e$ [11]. And the no-fly zone q with a circular horizontal cross-section whose center coordinates are represented by $\mathbf{w}_q = (x_q, y_q)^{\mathrm{T}}$. The flight altitude of UAV is fixed at H_U and the horizontal coordinate of UAV i is $\mathbf{w}_i[n] = (x_i[n], y_i[n])^{\mathrm{T}}$. The gridding model is used to divide the horizontal plane into square grids. [12].

The binary variables $a_{ij}[n]$, $b_{ie}[n]$ and $c_{ik}[n]$ are used to represent the different role-switching decisions of UAV i in time slot n. And binary variable l_{je} is also introduced to represent whether user j is eavesdropped by eavesdropper e, which satisfies the constraints $\sum l_{je} \le 1$ for all j and e .

A. Communication Model

Given the maximum horizontal communication distance of the UAV d_{com}^{max}, when H_U is greater than the threshold of the height, the line-of-sight probability of the wireless link between the UAV and the ground nodes within d_{com}^{max} is approximately 1 [13], and the free space path loss model is adopted. Therefore, the channel power gains of the UAV i with the user j and the eavesdropper e are expressed as follows:

$$g_{ij}[n] = \frac{\beta_0}{d_{ij}[n]^{\phi^{AG}}}, \forall n,i,j \text{ and } g_{ie}[n] = \frac{\beta_0}{d_{ie}[n]^{\phi^{AG}}}, \forall n,i,e \tag{1}$$

where $d_{ij}[n] = \sqrt{H_U^2 + \|\mathbf{w}_i[n] - \mathbf{w}_j\|^2}$, $d_{ie}[n] = \sqrt{H_U^2 + \|\mathbf{w}_i[n] - \mathbf{w}_e\|^2}$. And β_0 represents the channel power gain at a unit distance and ϕ^{AG} is the path loss exponent. The terrestrial wireless link employs small-scale Rayleigh fading and large-scale path loss. Therefore, the channel power gain between user j and eavesdropper e is expressed as:

$$g_{je} = \frac{\beta_0}{d_{je}^{\phi^{GG}}}\xi, \forall j,e \tag{2}$$

where $d_{je} = \sqrt{\|\mathbf{w}_j - \mathbf{w}_e\|^2}$. And ξ represents the Rayleigh fading coefficient that follows an exponential distribution with a mean value of 1 and $\phi^{GG} > 2$ is the path loss exponent.

According to the above-mentioned channel power gain, the communication capacity (bps/Hz) in time slot n is:

$$R_{rec}[n] = \sum_{i=1}^{I}\sum_{j=1}^{J} a_{ij}[n]\log_2\left(1 + \frac{p_j[n]g_{ij}[n]}{\sigma^2}\right), \forall n \tag{3}$$

where $p_j[n]$ is the transmission power of user j and σ^2 is the power of the additive white Gaussian noise. Similarly, the eavesdropping capacity in time slot n is:

$$R_{wtp}[n] = \sum_{j=1}^{J}\sum_{e=1}^{E} l_{je}\mathbb{E}_\xi\left\{\log_2\left(1 + \frac{p_j[n]g_{je}}{X_n + \sigma^2}\right)\right\}, \forall n \tag{4}$$

where $X_n = \sum_{i=1}^{I} b_{ie}[n]p_i[n]g_{ie}[n]$ and $\mathbb{E}_\xi\{.\}$ represents the mathematical expectation with respect to the random variable ξ. $p_i[n]$ represents the transmission power of UAV i's the artificial noise. According to the definition of the secrecy capacity in the physical layer security theory, the secrecy capacity of the system in time slot n is:

$$R_{sec}[n] = \frac{1}{J}\left[R_{rec}[n] - R_{wtp}[n]\right]^+, \forall n \tag{5}$$

where $[R]^+ \triangleq \max(R, 0)$.

B. Energy Consumption Model

The system only takes into account the propulsion energy consumption of the UAVs, and models the propulsion energy consumption of the UAVs as [14]:

$$P^{pro}(V) = P_0\left(1 + \frac{3V^2}{U_{tip}^2}\right) + P_1\left(\sqrt{1 + \frac{V^4}{4v_0^2}} - \frac{V^2}{2v_0^2}\right)^{\frac{1}{2}} + \frac{1}{2}d_0\rho s A V^3 \tag{7}$$

$$(\mathcal{P}0): \quad \max_{\mathcal{A},\mathcal{B},\mathcal{C},\mathcal{P},\mathcal{W}} \frac{1}{N}\sum_{n=1}^{N} R_{sec}[n] \tag{6}$$

$$\text{s.t.} \quad \text{C1}: \begin{cases} \text{I}: \sum_{j=1}^{J} a_{ij}[n] + \sum_{e=1}^{E} b_{ie}[n] \\ \qquad + \sum_{k=1}^{K} c_{ik}[n] \le 1, \forall n, i \\ \text{II}: \sum_{i=1}^{I} a_{ij}[n] \le 1, \forall n, j \\ \text{III}: \sum_{i=1}^{I} b_{ie}[n] \le 1, \forall n, e \\ \text{IV}: \sum_{i=1}^{I} a_{ij}[n] = \sum_{i=1}^{I}\sum_{e=1}^{E} l_{je} b_{ie}[n], \forall n, j \end{cases}$$

$$\text{C2}: \begin{cases} \text{I}: 0 \le p_i[n] \le P_U^{max}, \forall n, i \\ \text{II}: \frac{1}{N}\sum_{n=1}^{N} p_i[n] \le P_U^{avg}, \forall i \\ \text{III}: 0 \le p_j[n] \le P_{GU}^{max}, \forall n, j \\ \text{IV}: \frac{1}{N}\sum_{n=1}^{N} p_j[n] \le P_{GU}^{avg}, \forall j \end{cases}$$

$$\text{C3}: \begin{cases} \text{I}: \|\mathbf{w}_i[n] - \mathbf{w}_i[n-1]\|^2 \le l_{gri}^2, \forall n, i \\ \text{II}: \|\mathbf{w}_i[n] - \mathbf{w}_{i'}[n]\|^2 \ge (d_{saf}^{min})^2, \forall n \ne N, i \ne i' \\ \text{III}: \|\mathbf{w}_i[n] - \mathbf{w}_q\|^2 \ge r_{nfz}^2, \forall n, i, q \\ \text{IV}: \mathbf{w}_i[0] = \mathbf{w}_i^I \quad \mathbf{w}_i[N] = \mathbf{w}_i^F, \forall i \end{cases}$$

$$\text{C4}: \begin{cases} \text{I}: a_{ij}[n] \|\mathbf{w}_i[n] - \mathbf{w}_j\|^2 \le (d_{com}^{max})^2, \forall n, i, j \\ \text{II}: b_{ie}[n] \|\mathbf{w}_i[n] - \mathbf{w}_e\|^2 \le (d_{com}^{max})^2, \forall n, i, e \end{cases}$$

$$\text{C5}: \begin{cases} \text{I}: E_i^{rem}[n] \ge \eta E_U, \forall n, i \\ \text{II}: E_i^{rem}[0] = E_U, \forall i \end{cases}$$

$$\text{C6}: t_{hov}^{min} \sum_{n=1}^{N}\sum_{i=1}^{I} a_{ij}[n] \log_2\left(1 + \frac{p_j[n] g_{ij}[n]}{\sigma^2}\right) \ge D, \forall j$$

$$a_{ij}[n] \in \{0,1\}, \forall n, i, j \quad b_{ie}[n] \in \{0,1\}, \forall n, i, e$$

$$c_{ik}[n] \in \{0,1\}, \forall n, i, k$$

where V is the horizontal flight speed of the UAV, P_0 and P_1 are the blade profile energy and the induced energy of the UAV in the hovering state, U_{tip} represents the tip speed of the rotor blade, v_0 represents the average rotor-induced speed of UAV in the hovering state, d_0, ρ, s and A are the fuselage drag ratio, air density, rotor solidity and rotor disk area respectively. The energy consumption of UAV i at time slot n is:

$$E_i[n] = t_i^{pro}[n] P^{pro}(V) + t_i^{hov}[n] P^{pro}(0), \forall n, i \tag{8}$$

where $t_i^{pro}[n] = \|\mathbf{w}_i[n] - \mathbf{w}_i[n-1]\| / V$ is the propulsion time of UAV i and $t_i^{hov}[n] = \delta t - t_i^{pro}[n]$ is the hovering time. Therefore, the remaining energy is:

$$\begin{aligned} E_i^{rem}[n] =& (1 - \sum_{k=1}^{K} c_{ik}[n])(E_i^{rem}[n-1] - E_i[n]) \\ &+ \sum_{k=1}^{K} c_{ik}[n] E_U, \forall n, i \end{aligned} \tag{9}$$

where $E_i^{rem}[n-1]$ is the remaining energy at time slot $n-1$ and E_U is the battery capacity of the UAV.

C. Problem Formulation

Let $\mathcal{A} = \{a_{ij}[n], \forall n, i, j\}$ denote the set of communication reception decision variables for all UAVs, $\mathcal{B} = \{b_{ie}[n], \forall n, i, e\}$ denote the set of friendly jamming decision variables for all UAVs, $\mathcal{C} = \{c_{ik}[n], \forall n, i, k\}$ denote the set of energy replenishment decision variables for all UAVs, $\mathcal{P} = \{p_i[n], p_j[n], \forall n, i, j\}$ denote the set of all transmission power variables, and $\mathcal{W} = \{\mathbf{w}_i[n], \forall n, i\}$ denote the set of trajectory variables for all UAVs.

The objective is maximizing secrecy capacity in the worst case by jointly optimizing UAV role-switching decisions, power allocation strategies, and trajectory planning. The optimization deployment problem is formulated as equation (6). The non-smooth function caused by the operation of $[.]^+$, the mathematical expectation of ξ, and The uncertainty of eavesdropper positions makes solving the optimization problem difficult. The optimization variable $p_j[n]$ can be assigned a value of 0 if $R_{rec}[n] - R_{wtp}[n] < 0$. Therefore, $R_{sec}[n]$ is always non-negative through the optimization of $p_j[n]$. The operator $[.]^+$ can be omitted without changing the optimal solution of the original problem. In addition, we derive an upper bound:

$$\hat{R}_{wtp}[n] = \sum_{j=1}^{J}\sum_{e=1}^{E} l_{je} \log_2\left(1 + \frac{p_j[n]\hat{g}_{je}}{\hat{X}_n + \sigma^2}\right), \forall n \tag{10}$$

where $\hat{X}_n = \sum_{i=1}^{I} b_{ie}[n] p_i[n] \hat{g}_{ie}[n]$. Therefore, the original optimization problem is approximated as $\mathcal{P}1$:

$$(\mathcal{P}1): \quad \max_{\mathcal{A},\mathcal{B},\mathcal{C},\mathcal{P},\mathcal{W}} \frac{1}{N}\sum_{n=1}^{N}\left(R_{rec}[n] - \hat{R}_{wtp}[n]\right)$$

$$\text{s.t.} \quad \text{C1}, \text{C2}, \text{C3}, \text{C4}, \text{C5}, \text{C6}$$

$$a_{ij}[n] \in \{0,1\}, \forall n, i, j \quad b_{ie}[n] \in \{0,1\}, \forall n, i, e$$

$$c_{ik}[n] \in \{0,1\}, \forall n, i, k$$

III. Proposed Solution

Although the objective function of $\mathcal{P}1$ becomes easier to handle, it remains a non-convex optimization problem that is difficult to solve due to variable coupling and non-convex functions in both the objective function and constraints. This paper proposes an algorithm based on block coordinate descent (BCD) and successive convex approximation (SCA) to maximize the secrecy capacity.

A. Subproblem 1: Role Switching

Given the fixed transmission power and trajectory variables $\{\mathcal{P}, \mathcal{W}\}$, the UAV role-switching decision variables $\{\mathcal{A}, \mathcal{B}, \mathcal{C}\}$ are optimized by

$$(\mathcal{SP}1): \quad \max_{\mathcal{A},\mathcal{B},\mathcal{C}} \frac{1}{N}\sum_{n=1}^{N}\left(R_{rec}[n] - \hat{R}_{wtp}[n]\right)$$

$$\text{s.t.} \quad \text{C1}, \text{C4}, \text{C5}, \text{C6}$$

where $R_{rec}[n]$ is a linear function of $a_{ij}[n]$ in the objective function and let $X_n = \sum_{i=1}^{I} b_{ie}[n] p_i[n] \hat{g}_{ie}[n] + \sigma^2$. Using

the properties of logarithmic functions and binary variables, $\hat{R}_{wtp}[n]$ can be rewritten as:

$$\hat{R}_{wtp}[n] = \sum_{j=1}^{J}\sum_{e=1}^{E} l_{je} b_{ie}[n] \log_2\left(X_n\big|_{\sum_{i=1}^{I} b_{ie}[n]=1} + p_j[n]\hat{g}_{je}\right) + \sum_{j=1}^{J}\sum_{e=1}^{E} l_{je}(1-b_{ie}[n]) \log_2\left(X_n\big|_{\sum_{i=1}^{I} b_{ie}[n]=0} + p_j[n]\hat{g}_{je}\right) - \sum_{j=1}^{J}\sum_{e=1}^{E} l_{je}\log_2(X_n) \quad (11)$$

The objective function is a concave function with respect to $a_{ij}[n]$, $b_{ie}[n]$ and $c_{ik}[n]$, and the optimization problem can be solved using convex optimization toolboxes (such as CVX).

B. Subproblem 2: Power allocation

Based on the given UAV role-switching decision variables and trajectory variables $\{\mathcal{A}, \mathcal{B}, \mathcal{C}, \mathcal{W}\}$, the optimization of transmission power variables $\{\mathcal{P}\}$ can be formulated as

$$(\mathcal{SP}2): \quad \max_{\mathcal{P}} \frac{1}{N}\sum_{n=1}^{N}\left(R_{rec}[n] - \hat{R}_{wtp}[n]\right) \quad \text{s.t.} \quad \text{C2, C6}$$

Obviously, $R_{rec}[n]$ is a concave function of $p_j[n]$. Let $X_n = \sum_{i=1}^{I} b_{ie}[n]p_i[n]\hat{g}_{ie}[n]$ and using the properties of the logarithmic function, $-\hat{R}_{wtp}[n]$ can be rewritten as:

$$-\hat{R}_{wtp}[n] = \sum_{j=1}^{J}\sum_{e=1}^{E} l_{je}\log_2\left(X_n + \sigma^2\right) - \sum_{j=1}^{J}\sum_{e=1}^{E} l_{je}\log_2\left(X_n + p_j[n]\hat{g}_{je} + \sigma^2\right) \quad (12)$$

where $\log_2\left(X_n + \sigma^2\right)$ is a concave function of $p_i[n]$ and $\log_2\left(X_n + p_j[n]\hat{g}_{je} + \sigma^2\right)$ is a concave function of $p_i[n]$ and $p_j[n]$. Subtracting a concave function from another concave function is essentially in the form of adding a convex function to a concave function. Therefore, $-\hat{R}_{wtp}[n]$ is a non-convex function. Let $R_n = -\sum_{j=1}^{J}\sum_{e=1}^{E} l_{je}\log_2\left(X_n + p_j[n]\hat{g}_{je} + \sigma^2\right)$. Its global lower-bound function is obtained through the first-order Taylor expansion:

$$R_n \geq -\sum_{j=1}^{J}\sum_{e=1}^{E} l_{je}\log_2\left(X_n^0 + p_j^0[n]\hat{g}_{je} + \sigma^2\right) + \frac{(X_n - X_n^0) + \hat{g}_{je}(p_j[n] - p_j^0[n])}{\ln 2(X_n^0 + p_j^0[n]\hat{g}_{je} + \sigma^2)} \triangleq f_1(X_n, p_j[n]) \quad (13)$$

where $X_n^0 = \sum_{i=1}^{I} b_{ie}[n]p_i^0[n]\hat{g}_{ie}[n]$ is the value at an arbitrary feasible point $p_i^0[n]$ and $p_j[n]$ is an arbitrary feasible point of $p_j[n]$. Obviously, f_1 is an affine function of X_n and $p_j[n]$. The global lower-bound function of $-\hat{R}_{wtp}[n]$ is:

$$-\hat{R}_{wtp}^{ub}[n] \triangleq \sum_{j=1}^{J}\sum_{e=1}^{E} l_{je}\log_2\left(X_n + \sigma^2\right) + f_1(X_n, p_j[n]) \quad (14)$$

Based on the above, an approximate optimal solution is obtained by maximizing the global lower-bound function:

$$(\mathcal{SP}2'): \quad \max_{\mathcal{P}} \frac{1}{N}\sum_{n=1}^{N}\left(R_{rec}[n] - \hat{R}_{wtp}^{ub}[n]\right) \quad \text{s.t.} \quad \text{C2, C6}$$

C. Subproblem 3: Trajectory Plannning

To better align with practical application scenarios, the secrecy capacity minus the square of the distance is used to incentivize UAVs to replace batteries at stations. With the given UAV role-switching and transmission power variables $\{\mathcal{A}, \mathcal{B}, \mathcal{C}, \mathcal{P}\}$, the trajectory variables $\{\mathcal{W}\}$ are optimized by introducing the slack variables $\mathcal{S} = \{s_{ij}[n], \forall n, i, j\}$, $\mathcal{T} = \{t_{ie}[n], \forall n, i, e\}$ and $\mathcal{U} = \{u_{ik}[n], \forall n, i, k\}$:

$$(\mathcal{SP}3): \max_{\mathcal{W},\mathcal{S},\mathcal{T},\mathcal{U}} \frac{1}{N}\sum_{n=1}^{N}\left(R_{rec}[n] - \hat{R}_{wtp}[n] - c_{ik}[n]d_{ik}^2[n]\right)$$

s.t. C3, C4, C5, C6

$$\text{C7}: \begin{cases} \text{I}: \|\mathbf{w}_i[n] - \mathbf{w}_j\|^2 + H_U^2 \leq s_{ij}[n], \forall n, i, j \\ \text{II}: (\|\mathbf{w}_i[n] - \hat{\mathbf{w}}_e\| + r_{eve})^2 + H_U^2 \leq t_{ie}[n], \forall n, i, e \\ \text{III}: \|\mathbf{w}_i[n] - \mathbf{w}_k\|^2 \leq u_{ik}[n], \forall n, i, k \end{cases}$$

When the optimal solution of $\mathcal{SP}3$ is obtained, the equality of the convex constraint C7 with respect to $\mathbf{w}_i[n]$ holds. $R_{rec}[n]$ is a convex function with respect to $s_{ij}[n]$. Using the SCA method, the global lower-bound function of $R_{rec}[n]$ is obtained through the first-order Taylor expansion:

$$R_{rec}^{lb}[n] = \sum_{i=1}^{I}\sum_{j=1}^{J} a_{ij}[n]\log_2\left(1 + \frac{P_j[n]}{(s_{ij}^0[n])^{\frac{\phi^{AG}}{2}}}\right) - \sum_{i=1}^{I}\sum_{j=1}^{J} a_{ij}[n]\frac{\phi^{AG}P_j[n](s_{ij}[n] - s_{ij}^0[n])}{2\ln 2(s_{ij}^0[n])^{\frac{\phi^{AG}}{2}+1}\left(1 + \frac{P_j[n]}{(s_{ij}^0[n])^{\frac{\phi^{AG}}{2}}}\right)} \quad (15)$$

where $P_j[n] = \frac{p_j[n]\beta_0}{\sigma^2}$, $R_{rec}^{lb}[n]$ is an affine function of $s_{ij}[n]$ and $s_{ij}^0[n]$ is an arbitrary feasible point of $s_{ij}[n]$. Similarly, $\hat{R}_{wtp}[n]$ is a concave function with respect to $t_{ie}[n]$. Using the SCA method, the global upper-bound function of $\hat{R}_{wtp}[n]$ is obtained through the first-order Taylor expansion:

$$\hat{R}_{wtp}^{ub}[n] = \sum_{j=1}^{J}\sum_{e=1}^{E} l_{je}\log_2\left(1 + Y_n\big|_{t_{ie}[n]=t_{ie}^0[n]}\right) - \sum_{j=1}^{J}\sum_{e=1}^{E} l_{je}\frac{\phi^{AG}\sum_{i=1}^{I} b_{ie}[n]p_i[n]\beta_0 \cdot p_j[n]\hat{g}_{je}(t_{ie}^0[n])^{-\frac{\phi^{AG}}{2}-1}}{2\ln 2\left(1 + Y_n\big|_{t_{ie}[n]=t_{ie}^0[n]}\right)\left(Z_n\big|_{t_{ie}[n]=t_{ie}^0[n]}\right)^2} (t_{ie}[n] - t_{ie}^0[n]), \forall n \quad (16)$$

where $Y_n = \frac{p_j[n]\hat{g}_{je}}{Z_n}$ and $Z_n = \sum_{i=1}^{I} b_{ie}[n]p_i[n]\frac{\beta_0}{t_{ie}[n]^{\frac{\phi^{AG}}{2}}} + \sigma^2$. $\hat{R}_{wtp}^{ub}[n]$ is an affine function of $t_{ie}[n]$ and $t_{ie}^0[n]$ is an arbitrary feasible point of $t_{ie}[n]$. C3-II and C3-III are non-convex constraints. The SCA method is used to obtain the

first-order Taylor expansions of the convex functions.

$$f_2(\mathbf{w}_i[n]) \triangleq \left\|\mathbf{w}_i^0[n]-\mathbf{w}_{i'}[n]\right\|^2 + 2\left(\mathbf{w}_i^0[n]-\mathbf{w}_{i'}[n]\right)^{\mathrm{T}}\left(\mathbf{w}_i[n]-\mathbf{w}_i^0[n]\right) \quad (17)$$

$$f_3(\mathbf{w}_i[n]) \triangleq \left\|\mathbf{w}_i^0[n]-\mathbf{w}_q[n]\right\|^2 + 2\left(\mathbf{w}_i^0[n]-\mathbf{w}_q[n]\right)^{\mathrm{T}}\left(\mathbf{w}_i[n]-\mathbf{w}_i^0[n]\right) \quad (18)$$

Therefore, the C3 can be rewritten as

$$\mathrm{C3}': \begin{cases} \mathrm{I}: \|\mathbf{w}_i[n]-\mathbf{w}_i[n-1]\|^2 \le l_{gri}^2, \quad \forall n,i \\ \mathrm{II}: f_2(\mathbf{w}_i[n]) \ge (d_{saf}^{min})^2, \quad \forall n \ne N, i, i \ne i' \\ \mathrm{III}: f_3(\mathbf{w}_i[n]) \ge r_{nfz}^2, \quad \forall n,i,q \\ \mathrm{IV}: \mathbf{w}_i[0]=\mathbf{w}_i^I \quad \mathbf{w}_i[N]=\mathbf{w}_i^F, \quad \forall i \end{cases}$$

Additionally, C6 is also a non-convex constraint, and the function within it needs to be transformed into:

$$f_4(s_{ij}[n]) \triangleq t_{hov}^{min}\sum_{n=1}^{N}\sum_{i=1}^{I} a_{ij}[n]\log_2\left(1+\frac{P_j[n]}{(s_{ij}^0[n])^{\frac{\phi^{AG}}{2}}}\right) - t_{hov}^{min}\sum_{n=1}^{N}\sum_{i=1}^{I} a_{ij}[n]\frac{\phi^{AG}P_j[n](s_{ij}[n]-s_{ij}^0[n])}{2\ln 2(s_{ij}^0[n])^{\frac{\phi^{AG}}{2}+1}\left(1+\frac{P_j[n]}{(s_{ij}^0[n])^{\frac{\phi^{AG}}{2}}}\right)} \quad (19)$$

In this way, the constraint C6 can be rewritten as

$$\mathrm{C6}': f_4(s_{ij}[n]) \ge D, \quad \forall j$$

Since the two-dimensional coordinates of the system adopt a gridding model, by introducing an auxiliary variable $\mathcal{M}=\{\mathbf{m}_i[n],\forall n,i\}$, there is the constraint:

$$\mathrm{C8}: \begin{cases} \mathrm{I}: 1 \le \mathbf{m}_i[n] \le \frac{l_{sce}}{l_{gri}}, \quad \forall n,i \\ \mathrm{II}: \mathbf{w}_i[n]=\mathbf{m}_i[n]\cdot l_{gri}-\frac{l_{gri}}{2}, \quad \forall n,i \\ \mathbf{m}_i[n]\in\mathbb{Z}, \quad \forall n,i \end{cases}$$

Based on the above discussion, transform $\mathcal{SP}3$ into $\mathcal{SP}3'$:

$$(\mathcal{SP}3'): \max_{\mathcal{M},\mathcal{S},\mathcal{T},\mathcal{U}} \frac{1}{N}\sum_{n=1}^{N}\left(R_{rec}^{lb}[n]-\hat{R}_{wtp}^{ub}[n]-c_{ik}[n]u_{ik}[n]\right)$$
$$\text{s.t.} \quad \mathrm{C3}', \mathrm{C4}, \mathrm{C5}, \mathrm{C6}', \mathrm{C7}, \mathrm{C8}$$

So far, the three subproblems (namely $\mathcal{SP}1$, $\mathcal{SP}2$, and $\mathcal{SP}3$) can be iteratively solved to yield an approximate global optimal solution using BCD until the convergence is achieved.

IV. Numerical Results and Discussion

In the simulations, the specific parameters of the UAV refer to the DJI Mini 3 drone, including a battery capacity of 18.1 Wh, etc. Assume that the flight speed V is fixed at 40 m/s. Set $\delta t = 1.5$ s to ensure that the UAV can have a period of hovering time after moving in each time slot. Furthermore, the time for the UAV to replace the battery at the station midway should be reduced. Therefore, assume that the energy replenishment machine can complete two operations within each time slot. To maintain the line-of-sight probability in a suburban environment between the UAV and the ground nodes within the maximum horizontal communication distance d_{com}^{max} to be approximately 1, the elevation angle $\theta \ge 20°$. Therefore, H_U is assumed as $\tan(20°)\cdot d_{com}^{max} = 36.4$ m.

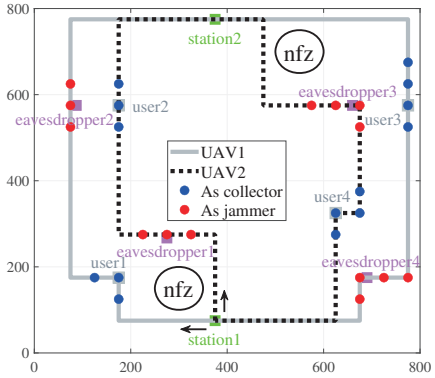

Fig. 2. An example of UAV trajectory planning results.

The comparison algorithms are described as follows: 1) *Non-Robust DOFJ (DOFJ-NR)*, in which the estimated eavesdropper location is accurate; 2) *Fixed-Role (FR)*, in which UAVs keep their initial roles without dynamic switching during flight; 3) *Fixed-Power (FP)*, where the transmission power of users and UAVs in each time slot always equals their respective specified average transmission power; 4) *Fixed-Trajectory (FT)*, where UAVs move according to the predefined flight trajectory.

Fig. 2 illustrates the flight trajectories of UAVs under the DOFJ algorithm. Starting from Station 1, two UAVs bypass the no-fly zone, recharge at Station 2 before energy depletion, and return to Station 1. By accounting for eavesdropper location uncertainty, DOFJ enables friendly jammers to approach eavesdroppers more closely. Moreover, dynamic role switching shortens UAVs' flight distances to users and eavesdroppers, enhancing secure communication duration.

Fig. 3(a) depicts the relationship between secrecy capacity and the maximum user's transmission power. For the FP algorithm, as its transmit power remains at the average value, it is unaffected. Other algorithms show an overall upward trend in secrecy capacity, as higher user transmit power boosts data reception capacity. However, when P_{GU}^{max} surpasses 30 dBm, the secrecy capacity saturates. Due to nearby eavesdroppers, excessive transmit power risks increased eavesdropping, prompting users to cap their power. Fig. 3(b) shows the relationship between secrecy capacity and the maximum UAV's transmission power. As before, the FP algorithm is unaffected as its transmit power stays at the average. Other algorithms generally see an upward trend in secrecy capacity as greater UAV transmit power reduces eavesdropping capacity. However, when P_U^{max} exceeds 35 dBm, the secrecy capacity saturates. Due to full-power jamming by the UAV, the marginal effect leads to a slower growth rate.

Fig. 3(c) illustrates the relationship between secrecy capacity and the uncertain area radius of eavesdroppers. DOFJ, FR, and FP optimize their flight paths to handle worsening eavesdropping, resulting in gentle downward trends. In contrast, FT's fixed trajectory is less effective against eavesdropping, causing a sharper decline. Since DOFJ-NR ignores eavesdropper position uncertainty, its trajectory op-

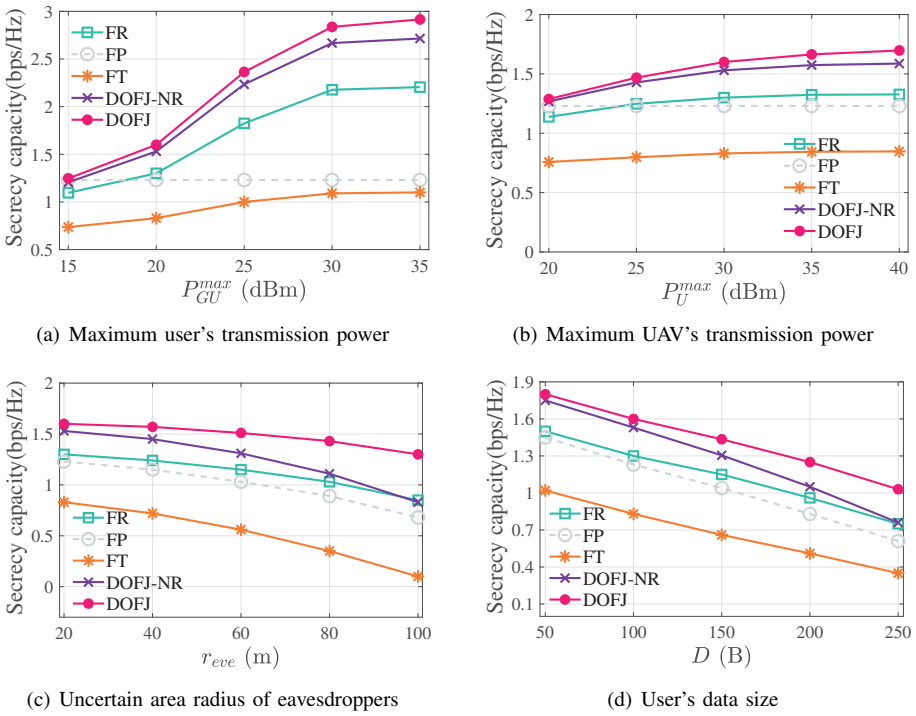

(a) Maximum user's transmission power

(b) Maximum UAV's transmission power

(c) Uncertain area radius of eavesdroppers

(d) User's data size

Fig. 3. Performance comparison in terms of secrecy capacity.

timization avoids worst-case eavesdropping, reducing robustness. Fig. 3(d) shows the relationship between secrecy capacity and the user's data size. As data volume rises, secrecy capacity drops because UAVs must hover longer near users in high-eavesdropping areas to complete data reception. In DOFJ-NR and FT, lacking optimal hovering positions, and in FP with sub-optimal transmit power, the extended hovering time near vulnerable user-eavesdropper pairs accelerates the decline in secrecy capacity. The proposed DOFJ algorithm maintains the best overall system performance.

V. Conclusions

This paper proposes an optimization deployment algorithm to maximize secrecy capacity under worst-case scenarios. Using time discretization, the problem models multi-UAV systems with dynamic role switching, establishing decision-making, communication, and energy models. An optimization problem is formulated under constraints on UAV trajectories, power, and battery levels. Due to non-convexity and variable coupling, algorithm based on BCD and SCA is designed. Simulations show that the proposed DOFJ exhibits superior secrecy capacity performance across various scenarios.

References

[1] Y. Zeng, R. Zhang, and T. J. Lim, "Wireless communications with unmanned aerial vehicles: opportunities and challenges," *IEEE Commun. Mag.*, vol. 54, no. 5, pp. 36–42, 2016.

[2] L. Xiao, H. Li, S. Yu, Y. Zhang, L.-C. Wang, and S. Ma, "Reinforcement learning based network coding for drone-aided secure wireless communications," *IEEE Trans. Commun.*, vol. 70, no. 9, pp. 5975–5988, 2022.

[3] D. Kapetanovic, G. Zheng, and F. Rusek, "Physical layer security for massive mimo: An overview on passive eavesdropping and active attacks," *IEEE Commun. Mag.*, vol. 53, no. 6, pp. 21–27, 2015.

[4] H. Kang, X. Chang, J. Mišić, V. B. Mišić, J. Fan, and J. Bai, "Improving dual-uav aided ground-uav bi-directional communication security: Joint uav trajectory and transmit power optimization," *IEEE Trans. on Veh. Technol.*, vol. 71, no. 10, pp. 10 570–10 583, 2022.

[5] R. Zhang, X. Pang, W. Lu, N. Zhao, Y. Chen, and D. Niyato, "Dual-uav enabled secure data collection with propulsion limitation," *IEEE Trans. on Wireless Commun.*, vol. 20, no. 11, pp. 7445–7459, 2021.

[6] X. Hou, J. Wang, C. Jiang, X. Zhang, Y. Ren, and M. Debbah, "Uav-enabled covert federated learning," *IEEE Trans. on Wireless Commun.*, vol. 22, no. 10, pp. 6793–6809, 2023.

[7] H. Fu, Z. Sheng, A. A. Nasir, A. H. Muqaibel, and L. Hanzo, "Securing the uav-aided non-orthogonal downlink in the face of colluding eavesdroppers," *IEEE Trans. on Veh. Technol.*, vol. 71, no. 6, pp. 6837–6842, 2022.

[8] R. Shakeri, M. A. Al-Garadi, A. Badawy, A. Mohamed, T. Khattab, A. K. Al-Ali, K. A. Harras, and M. Guizani, "Design challenges of multi-uav systems in cyber-physical applications: A comprehensive survey and future directions," *IEEE Commun. Surv. & Tut.*, vol. 21, no. 4, pp. 3340–3385, 2019.

[9] H. Hong, Y. Zhang, and Y. Xie, "Energy-limited uav visiting planning for age-aware wireless-powered sensor networks," in *2023 IEEE 98th Vehicular Technology Conference (VTC2023-Fall)*, 2023, pp. 1–6.

[10] D. Deng, W. Zhou, X. Li, D. B. da Costa, D. W. K. Ng, and A. Nallanathan, "Joint beamforming and uav trajectory optimization for covert communications in isac networks," *IEEE Trans. on Wireless Commun.*, vol. 24, no. 2, pp. 1016–1030, 2025.

[11] Y. Cai, Z. Wei, R. Li, D. W. K. Ng, and J. Yuan, "Joint trajectory and resource allocation design for energy-efficient secure uav communication systems," *IEEE Trans. on Commun.*, vol. 68, no. 7, pp. 4536–4553, 2020.

[12] E. Eldeeb, J. M. d. S. Sant'Ana, D. E. Pérez, M. Shehab, N. H. Mahmood, and H. Alves, "Multi-uav path learning for age and power optimization in iot with uav battery recharge," *IEEE Trans. on Veh. Technol.*, vol. 72, no. 4, pp. 5356–5360, 2023.

[13] A. Al-Hourani, S. Kandeepan, and S. Lardner, "Optimal lap altitude for maximum coverage," *IEEE Wireless Commun. Lett.*, vol. 3, no. 6, pp. 569–572, 2014.

[14] G. Chen, X. B. Zhai, and C. Li, "Joint optimization of trajectory and user association via reinforcement learning for uav-aided data collection in wireless networks," *IEEE Trans. on Wireless Commun.*, vol. 22, no. 5, pp. 3128–3143, 2023.